Acknowledgements

We thank A. Nicholls for discussions and help with TEM analysis. The work done at UIC was supported by the US NSF, and the work done at Drexel University was supported by DARPA via ONR contract. The electron microscopes used in this work are operated by the Research Resources Center at UIC. The JEM-2010F purchase was supported by the NSF.

Correspondence and requests for materials should be addressed to Y.G. (e-mail: gogotsi@drexel.edu).

A 300-million-year record of atmospheric carbon dioxide from fossil plant cuticles

Gregory J. Retallack

Department of Geological Sciences, University of Oregon, Eugene, Oregon 97403-1272, USA

To understand better the link between atmospheric CO_2 concentrations and climate over geological time, records of past CO_2 are reconstructed from geochemical proxies[1–4]. Although these records have provided us with a broad picture of CO_2 variation throughout the Phanerozoic eon (the past 544 Myr), inconsistencies and gaps remain that still need to be resolved. Here I present a continuous 300-Myr record of stomatal abundance from fossil leaves of four genera of plants that are closely related to the present-day *Ginkgo* tree. Using the known relationship between leaf stomatal abundance and growing season CO_2 concentrations[5,6], I reconstruct past atmospheric CO_2 concentrations. For the past 300 Myr, only two intervals of low CO_2 (<1,000 p.p.m.v.) are inferred, both of which coincide with known ice ages in Neogene (1–8 Myr) and early Permian (275–290 Myr) times. But for most of the Mesozoic era (65–250 Myr), CO_2 levels were high (1,000–2,000 p.p.m.v.), with transient excursions to even higher CO_2 (>2,000 p.p.m.v.) concentrations. These results are consistent with some reconstructions of past CO_2 (refs 1, 2) and palaeotemperature records[7], but suggest that CO_2 reconstructions based on carbon isotope proxies[3,4] may be compromised by episodic outbursts of isotopically light methane[8,9]. These results support the role of water vapour, methane and CO_2 in greenhouse climate warming over the past 300 Myr.

As atmospheric CO_2 levels have risen over the past 200 years of industrial fossil fuel consumption, plants have responded by decreasing the density of stomates on their leaves[5,6]. Here I use the well-known inverse relationship between atmospheric CO_2 concentration and stomatal density as a palaeobarometer of atmospheric CO_2 during growth of fossil plant leaves. Stomatal density of living plants has, however, been shown to be related to differences in insolation, water stress and stomatal position within leaves, which also affect cell size, and thus stomatal density. The effects of these competing variables are minimized by using stomatal index (percentage stomates over stomates plus epidermal cells) rather than stomatal density (stomates per unit area[6]). Further limits to such competing variables are suggested by the habitats of the fossil leaves studied: these were mostly humid, lowland, fluvial and swamp environments suitable for preservation of fossil plant cuticles[10]. The plants had nutrient-poor peaty and siliceous substrates, suffered periodic flood disturbance and were in open vegetation early in the ecological succession after disturbance, as is indicated by sedimentological and taphonomic studies of several of the studied fossil sites[10,11]. Another potentially misleading effect is the differences between trees of different sex in *Ginkgo*: pollen-producing trees

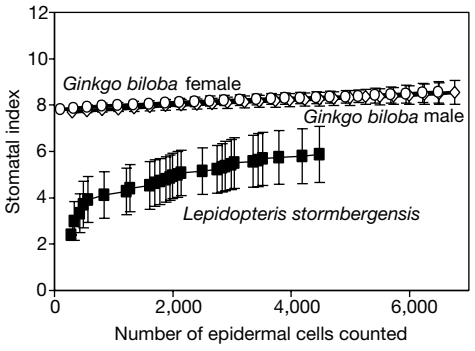

Figure 1 Rarefaction analysis indicates how many cells need to be counted for reliable determination of stomatal index (SI). Shown here are leaves of a female (circles) and male (diamonds) tree of *Ginkgo biloba* collected from Eugene, Oregon, 5 September 2000, and of *Lepidopteris stormbergensis* from the late Triassic (Carnian) Molteno formation at Little Switzerland, South Africa[12]. The *Ginkgo* samples were ideal: images of the same size from different leaves of two trees. The *Lepidopteris* samples were numerous but far from ideal: images of irregular shape and varied size, with great natural variation in SI, and from an unknown number of leaves or plants.

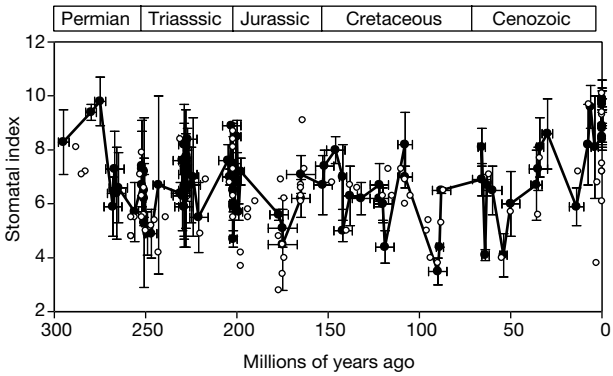

Figure 2 Stomatal index has varied considerably over the past 300 million years, but was as high during the early Permian ice age as it has been during the Neogene. Data are from fossil leaves of *Rhachiphyllum* (early Permian, 295–265 Myr ago), *Lepidopteris* (mid-Permian to late Triassic, 258–200 Myr ago), *Tatarina* (late Permian, 252–250 Myr ago) and *Ginkgo* (late Triassic to recent, 229–0 Myr ago). Filled symbols and the solid line are reliable data as established by rarefaction analysis (Fig. 1); unfilled symbols are statistically inadequate samples, and are plotted to show proven data density of the cuticular record of these taxa. All data are available as Supplementary Information.

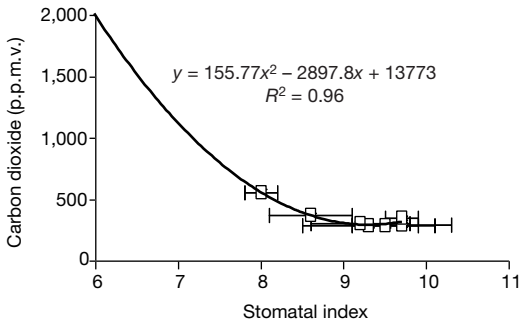

Figure 3 Palaeoatmospheric CO_2 can be inferred from fossil leaf SI by using this transfer function derived from *Ginkgo* leaves grown in greenhouse experiments[5] and taken from herbarium sheets dating back to 1888 (see Supplementary Information).

have branches reaching upwards and so are more evenly lit, whereas horizontal branches tend to shade lower branches in ovule-producing trees. Counts of stomatal index from SEM images of leaves of a male and female tree from Eugene, Oregon, showed identical stomatal index (mean SI was 8.6 ± 0.4; Fig. 1).

The most serious obstacle to the use of SI as a CO_2 palaeobarometer has been the different SI among species growing in the same location. For this reason, applications of this technique have focused on particular species, such as *Quercus petraea*, known in the fossil record back to the Miocene (10 Myr ago)[6]. Here I used primarily the genus *Ginkgo*, which has a fossil record of well-preserved leaf cuticles at least back to the late Triassic period (229 Myr ago)[12]. To extend this record back into the Palaeozoic, the pteridosperm genera *Lepidopteris* (Permian–Triassic), *Tatarina* (late Permian), and *Rhachiphyllum* (Permian) were chosen for several reasons. They have similar SI where they occur in the same places: for example, *Ginkgo telemachus* (SI 7.6 ± 1.4) and *Lepidopteris africana* (SI 6.5 ± 1.7) at Little Switzerland (late Triassic, South Africa[12]), and *Tatarina conspicua* (SI 5.5 ± 1.1) and *Lepidopteris* sp. (SI 6.3 ± 0.9) at Baizovka (late Permian, Russia[13]). Furthermore, there is a phylogenetic relationship between ginkgos and peltasperm seed ferns, as revealed by analysis of their fossilized reproductive structures[10]. All four genera also have morphologically similar stomates. Their subsidiary cell cuticles are darker (because they are thicker) than those of other epidermal cells. Subsidiary cells that are arranged in an even ring each have a hollow papilla oriented partly to occlude the stomatal pit. This kind of stomate is also found in cycads such as *Dioon*, and conifers such as *Torreya*, *Agathis* and *Thuja*[14]. Such partial papillar occlusion gives the stomatal apparatus of *Ginkgo*, *Lepidopteris*, *Tatarina*, and *Rhachiphyllum* a degree of functional equivalence that is not found in other fossil genera such as *Dicroidium*, *Pachypteris*, or *Baiera*[12].

This study used previously published illustrations of fossil cuticle (see Methods), with the exception of two early Triassic (250–245 Myr ago) species from near Sydney, Australia (see Supplementary Information). The numerical ages of the fossil cuticles were taken from a current geological time scale[15], but relative age came from published accounts of the cuticles. My compilation demonstrates that SI in Permian (275–296 Myr ago) *Rhachiphyllum* and *Lepidopteris* was comparable with Neogene (0–8 Myr ago) *Ginkgo*. Such high SI (>9) reflects low levels of atmospheric CO_2, predicted for the Permian by sedimentary mass balance models[1]. Cool climates would be predicted from the role of CO_2 as a greenhouse gas[5], and both the Neogene and the Permian are known from evidence of tillites, striated pavements, and ice-rafted debris to be times of large global ice caps[11]. These two end-points (Fig. 2) indicate that Permian plants were similar to modern ones in their relationship between stomatal index and atmospheric CO_2, and that there has not been long-term drift in this proxy measure of atmospheric CO_2.

Fossil plant cuticular SI can be calibrated to atmospheric CO_2 levels from greenhouse experiments using living *Ginkgo biloba*[5], which have shown SI 9.7 ± 0.2 at 350 p.p.m.v. and SI 8.0 ± 0.2 at 560 p.p.m.v. CO_2. Herbarium specimens of *Ginkgo biloba* ranging back in age to 1888 were also counted for stomatal index (see Supplementary Information), and CO_2 levels for each taken from global estimates for their year of collection[6]. Herbarium and green-

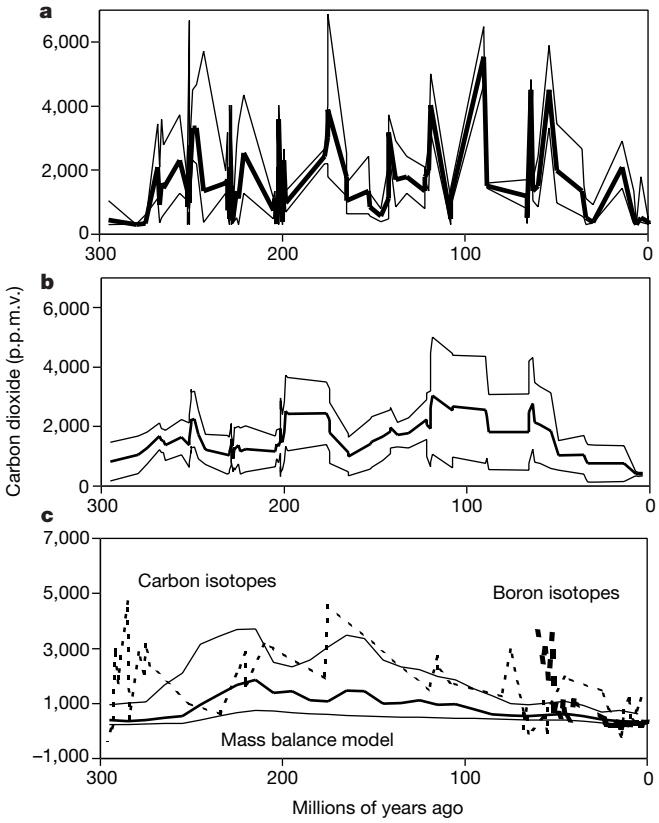

Figure 4 Cuticular estimates (**a**, **b**) of atmospheric CO_2 (p.p.m.v.) can be compared with other proxies (**c**) over the past 300 million years. **a**, Unsmoothed data using transfer function (Fig. 3) on mean and standard deviation of 84 reliable SI determinations of fossil plants (Fig. 2). **b**, Five-point moving average of transformed SI determinations with flanking standard error of means. **c**, Previously published curves derived from a sedimentary mass balance model[1] (thick line), boron isotopic composition of marine foraminifera[2] (bold dashed line) and carbon isotopic composition of pedogenic carbonate[3] (dashed line).

house results, together with additional greenhouse studies in progress[16], indicate that the response of SI to CO_2 concentrations is markedly nonlinear. Greenhouse[5] and herbarium data were fitted with a quadratic equation for the concentration of CO_2: $[CO_2] = 155.77\,(SI)^2 - 2897.8\,(SI) + 13773$, where $r^2 = 0.96$ (adjusted to sample size of 8). This transfer function (Fig. 3) was then used to estimate past partial pressures of CO_2 from individual SI measurements (Fig. 4a) and smoothed by a five-point moving average to give a curve (Fig. 4b) comparable to past estimates of atmospheric CO_2 (Fig. 4c).

Comparison of the new results with mass balance model estimates (Fig. 4c) is good, given the coarse resolution (10 Myr intervals) of the model compared with the present study (mean sample gap 3.6 ± 5.4 Myr). Cuticular estimates also show high CO_2 levels during the early Tertiary comparable to those by high-resolution (mean sample gap 1.8 ± 2.7 Myr) boron isotopic studies of marine foraminifera (Fig. 4c), although these estimates could be substantially reduced by correction for secular changes in riverine boron input to the ocean[17]. The increased warmth and weathering during times of high CO_2 demonstrated here is supported by evidence from petrographic and chemical studies of palaeosols[11,18], the migration of thermophilic organisms to high latitudes[8,11], and oxygen isotopic analyses of marine skeletal remains from different palaeolatitudes[7,8]. There are also indications from palaeosols and from palynology that times of high CO_2 were times of humid palaeoclimate, and conversely that cool intervening intervals were dry. For example, the abundance of fossil pollen that is taken as evidence of aridity in many parts of Asia[19] rises at all four times of low CO_2 and cooling during the Jurassic and Cretaceous (Fig. 4b). The low CO_2 and cooling from Eocene to Oligocene epochs that is indicated by the cuticular record (Fig. 4b) is matched by evidence for synchronous palaeoclimatic drying in the palaeosol record of central and western North America[18].

The cuticular time series (Fig. 4b) shows numerous transient excursions to very high CO_2 (>2,000 p.p.m.v.). High-resolution studies of the SI minimum in fossil *Ginkgo* and cycad leaves across the Triassic–Jurassic boundary (200 Myr ago; ref. 20) in Greenland and Sweden indicates a transient CO_2 spike coincident with excursion to isotopically lighter carbon ($\delta^{13}C_{org}$) of the same leaves, and mass extinction (claiming *Lepidopteris* among others)[21]. Other CO_2 and carbon isotopic transients following mass extinction of the earliest Triassic (250 Myr ago), and faunal overturn of the early Jurassic period (190 Myr ago), early Cretaceous period (117 Myr ago) and late Palaeocene epoch (55 Myr ago), have been related to catastrophic outbursts of isotopically light methane from permafrost and marine hydrate reservoirs[8,9,22]. Yet another CO_2 spike at the Cretaceous–Tertiary boundary is coincident with an excursion to lighter carbon isotopic values on land and in the sea, asteroid impact in Yucatan, and the mass extinctions that claimed dinosaurs and ammonites[23]. Transient CO_2 maxima in the cuticular time series (Fig. 4a, b) represent strong perturbations of the carbon cycle.

There are significant discrepancies between cuticular estimates of atmospheric CO_2 (Fig. 4a, b) and estimates based on the carbon isotopic composition of palaeosol carbonates (Fig. 4c), which indicate CO_2 minima (including even negative concentrations) at 250 Myr ago (earliest Triassic), 190 Myr ago (early Jurassic), 117 Myr ago (early Cretaceous) and 55 Myr ago (latest Palaeocene)[3]. The timing of these events may be a clue to reasons for the discrepancies, because carbon isotopic studies indicate that these were times of catastrophic release of isotopically light methane from permafrost and marine gas-hydrate reservoirs[8,9,22]. Once in the atmosphere, methane is oxidized within 2–7 years to carbon dioxide, which retains the unusual isotopic signature of gas-hydrate reservoirs isolated from global surficial systems[24]. Atmospheric additions of isotopically light methane may also explain why the palaeosol isotopic palaeobarometer[3] and high-resolution carbon isotopic studies of deep oceanic organic matter[4] failed to detect the high CO_2 levels and warm palaeoclimate of the middle Miocene, which is evident from the few Miocene results presented here (Figs 2, 4a, b), as well as from studies of foraminifera[25], plants[26], palaeosols[27] and oxygen isotopic composition of marine shells[7,25]. The observation that carbon isotopic palaeobarometers fail to show high CO_2 at times of warm palaeoclimate has led to the suggestion that climatic warming and increasing atmospheric CO_2 concentrations were decoupled[7,28]. If carbon isotopic CO_2 palaeobarometers are compromised by episodic methane outbursts, as suggested here, then the accepted role of CO_2, methane and water vapour as greenhouse gases remains intact for at least the past 300 million years[7]. □

Methods

Counts were made by marking photocopies of microphotographs of cuticles taken either in plain unpolarized light or from the SEM, which is preferable to light microphotographs of species with thin cuticles such as living *Ginkgo biloba*[29]. Although this meta-analysis has the advantage of relying almost entirely on data available in the public domain, a disadvantage is that many published cuticular studies illustrate insufficient cuticle for statistically adequate determination of SI (see Supplementary Information). Rarefaction analysis was used to determine which counts were reliable. Individual determinations of SI from different illustrated cuticle fragments were arranged in order from lowest to highest and cumulative means and standard deviations were computed and plotted against numbers of epidermal cells counted. Mean SI from counting 500 epidermal cells was a good approximation of mean SI after counting 6,000 epidermal cells (Fig. 1). The accuracy of SI estimates is comparable to that of point counting the percentage mineral composition of petrographic thin sections, for which 500 points is routine, but larger counts are needed for high-precision work[30]. Using the criterion of more than 500 epidermal cells gave 84 reliable SI measurements within the past 300 million years (not counting modern leaves). Open symbols in Fig. 2 show an additional 74 estimates based on less than 500 counted epidermal cells, and demonstrate the potential for published fossil plant cuticles to improve temporal resolution from a mean time gap between samples of 3.6 ± 5.4 Myr to 1.7 ± 2.7 Myr.

Received 13 November 2000; accepted 22 March 2001.

1. Berner, R. A. The rise of plants and their effect on weathering and atmospheric CO_2. *Science* **276,** 543–546 (1997).
2. Pearson, P. N. & Palmer, M. R. Atmospheric carbon dioxide concentrations over the past 60 million years. *Nature* **406,** 695–699 (2000).
3. Ekart, D. P., Cerling, T. E., Montañez, I. P. & Tabor, N. J. A 400 million year carbon isotope record of pedogenic carbonate: implications for paleoatmospheric carbon dioxide. *Am. J. Sci.* **299,** 805–827 (1999).
4. Pagani, M., Freeman, K. H. & Arthur, M. A. Late Miocene atmospheric CO_2 concentration and expansion of C_4 grasses. *Science* **285,** 876–879 (1999).
5. Beerling, D. J., McElwain, J. C. & Osborne, C. P. Stomatal responses of the "living fossil" *Ginkgo biloba* L. To changes in atmospheric CO_2 concentrations. *J. Exp. Bot.* **49,** 1603–1607 (1998).
6. Kürschner, W. M., van der Burgh, J., Visscher, H. & Dilcher, D. L. Oak leaves as biosensors of late Neogene and early Pleistocene paleoatmospheric CO_2 concentrations. *Mar. Micropaleont.* **27,** 299–312 (1996).
7. Veizer, J., Godderis, Y. & François, L. M. Evidence for decoupling of atmospheric CO_2 and global climate during the Phanerozoic eon. *Nature* **408,** 698–701 (2000).
8. Thomas, E., Zachos, J. C. & Bralower, T. J. in *Warm Climates in Earth History* (eds Huber, B. T., MacLeod, K. G. & Wing, S. L.) 132–160 (Cambridge Univ. Press, Cambridge, 2000).
9. Krull, E. S., Retallack, G. J., Campbell, H. J. & Lyon, G. L. $\delta^{13}C_{org}$ chemostratigraphy of the Permian-Triassic boundary in the Maitai Group, New Zealand: evidence for high-latitudinal methane release. *NZ J. Geol. Geophys.* **43,** 21–32 (2000).
10. Meyen, S. V. *Fundamentals of Palaeobotany* (Chapman & Hall, London, 1987).
11. Retallack, G. J. Postapocalyptic greenhouse revealed by earliest Triassic paleosols in the Sydney Basin, Australia. *Geol. Soc. Am. Bull.* **111,** 52–70 (1999).
12. Anderson, J. M. & Anderson, H. M. *Palaeoflora of Southern Africa, Molteno Formation (Triassic)* Vol. 2 *Gymnosperms (excluding* Dicroidium*)* (Balkema, Rotterdam, 1989).
13. Gomankov, A. V. & Meyen, S. V. *Tatarinovaya flora (soslav i rasprostranenie v pozdnei permi Evrazi) [Tatarian flora (composition and distribution in the late Permian of Eurasia)].* (Trudy Akademia Nauk SSSR 401, 1986).
14. Florin, R. Untersuchungen zur stammesgeschichte der Coniferales und Cordaitales. *K. Svenska Vet. Akad. Handl.* **10(1),** 1–588 (1931).
15. Gradstein, F. M. *et al.* in *Geochronology, Time Scales and Global Stratigraphic Correlation* (eds Berggren, W. A., Kent, D. V., Aubry, M.-P. & Hardenbol, J.) 95–126 (Spec. Pap. 54, Soc. Econ. Paleont. Mineral., Tulsa, 1995).
16. Royer, D. L., Berner, R. A. & Hickey, L. J. Estimating latest Cretaceous and early Tertiary atmospheric pCO_2 from stomatal indices. *Geol. Soc. Am. Abstr.* **32(7),** A196 (2000).
17. Lemarchand, D., Gaillardet, J., Lewin, E. & Allègre, C. J. The influence of rivers on marine boron isotopes and implications for reconstructing past ocean pH. *Nature* **408,** 951–954 (2000).
18. Retallack, G. J., Bestland, E. A. & Fremd, T. Eocene and Oligocene paleosols in central Oregon. *Geol. Soc. Am. Spec. Pap.* **344,** 1–192 (2000).
19. Vakrameev, V. A. *Jurassic and Cretaceous Floras and Climates of the Earth* 53 (Cambridge Univ. Pres, Cambridge, 1991).
20. Pálfy, J. *et al.* Timing the end-Triassic mass extinctions: first on land, then in the sea. *Geology* **28,** 39–42 (2000).
21. McElwain, J. C., Beerling, D. J. & Woodward, F. I. Fossil plants and global warming at the Triassic–Jurassic boundary. *Science* **285,** 1386–1390 (1999).

22. Jahren, A. H., Arens, N. C., Sarmiento, G., Guerro, J. & Amundson, R. Terrestrial record of methane hydrate dissociation in the Early Cretaceous. *Geology* **29,** 159–162 (2001).
23. Arens, N. C. & Jahren, A. H. Carbon isotope excursion in atmospheric CO_2 at the Cretaceous-Tertiary boundary: evidence from terrestrial sediments. *Palaios* **15,** 314–322 (2000).
24. Khalil, M. A. K. (ed.) *Atmospheric Methane* 86 (Springer, Berlin, 2000).
25. McGowran, B. & Li, Q.-Y. Miocene climatic oscillation recorded in the Lakes Entrance oil shaft, southern Australia. *Aust. J. Earth Sci.* **43,** 129–148 (1997).
26. Utescher, T., Mossbrugger, U. & Ashraf, A. R. Terrestrial climate evolution in northwest Germany over the last 25 million years. *Palaios* **15,** 430–449 (2000).
27. Schwartz, T. Lateritic bauxite in central Germany and implications for Miocene palaeoclimates. *Palaeogeogr. Palaeoclimatol. Palaeoecol.* **129,** 37–50 (1997).
28. Cowling, S. A. Plants and temperature: CO_2 uncoupling. *Science* **285,** 1500–1501 (1999).
29. McElwain, J. C. & Chaloner, W. C. The fossil cuticle as a skeletal record of environmental change. *Palaios* **11,** 376–388 (1996).
30. Retallack, G. J. *A Colour Guide to Paleosols* 117 (Wiley, Chichester, 1997).

Supplementary information is available on *Nature*'s World-Wide Web site (http://www.nature.com) or as paper copy from the London editorial office of *Nature*.

Acknowledgements

A. Liston provided herbarium specimens of *Ginkgo*, M. Shaffer helped with SEM imaging, and S. Tanaka supplied Japanese literature. W. Kürschner, D. Dilcher, S. Scheckler and V. Wilde offered useful botanical discussion. M. Manga and J. Wynn helped with curve fitting and diffusion equations.

Correspondence and requests for materials should be addressed to the author (e-mail: gregr@darkwing.uoregon.edu).

Strong coherence between solar variability and the monsoon in Oman between 9 and 6 kyr ago

U. Neff*, S. J. Burns†‡, A. Mangini*, M. Mudelsee§, D. Fleitmann† & A. Matter†

* *Heidelberg Academy of Sciences, Im Neuenheimer Feld 229, Heidelberg, Germany D-69120*
† *Geological Institute, University of Bern, Baltzerstrasse 1, Bern, Switzerland CH-3012*
§ *Institute of Meteorology, University of Leipzig, Stephanstrasse 3, Leipzig, Germany D-04103*

Variations in the amount of solar radiation reaching the Earth are thought to influence climate, but the extent of this influence on timescales of millennia to decades is unclear. A number of climate records show correlations between solar cycles and climate[1], but the absolute changes in solar intensity over the range of decades to millennia are small[2] and the influence of solar flux on climate is not well established. The formation of stalagmites in northern Oman has recorded past northward shifts of the intertropical convergence zone[3], whose northward migration stops near the southern shoreline of Arabia in the present climate[4]. Here we present a high-resolution record of oxygen isotope variations, for the period from 9.6 to 6.1 kyr before present, in a Th–U-dated stalagmite from Oman. The $\delta^{18}O$ record from the stalagmite, which serves as a proxy for variations in the tropical circulation and monsoon rainfall, allows us to make a direct comparison of the $\delta^{18}O$ record with the $\Delta^{14}C$ record from tree rings[5], which largely reflects changes in solar activity[6,7]. The excellent correlation between the two records suggests that one of the primary controls on centennial- to decadal-scale changes in tropical rainfall and monsoon intensity during this time are variations in solar radiation.

The Indian Ocean monsoon is one of the main weather systems on Earth, and variations in its intensity have broad oceanographic and economic effects. To date, studies of how and why the monsoon varies through time have been restricted to studies of meteorological records, which extend back about 150 years[8], or studies of lacustrine and marine sediments[9–12], which mainly yield information on millennial and longer timescales. At present, information on monsoon variation on decadal to centennial timescales is limited to identification of 'centennial-scale' changes in sedimentary records[13,14], but these studies lack the resolution to determine specific periodicities or forcing mechanisms. We have developed a high-resolution proxy for estimating variation in monsoon intensity by measuring past changes in $\delta^{18}O$ of monsoon rainfall as recorded in calcite $\delta^{18}O$ of a stalagmite.

Hoti cave is located in northern Oman on the southwestern side of the Oman mountains (57° 21′ E, 23° 05′ N, 800 m above sea level). The modern climate of the area is arid to semi-arid, and the area is not at present affected by the Indian Ocean monsoon system. However, numerous marine and continental palaeoclimate records indicate that the summer monsoon was considerably stronger during early to middle Holocene times than it is at present[9–12,15], accompanied by a shift in the northern limit of the monsoon rainfall belt far north of its modern location[15,16], which resulted in a continental pluvial period in the Sahel region of Africa, in Arabia and in India. In Hoti cave[3], the pluvial period led to deposition of a set of large stalagmites.

Here we present a high-resolution profile of $\delta^{18}O$ of stalagmite H5 from Hoti cave[3] on an improved timescale dated with 12 Th–U ages measured using mass spectrometry (see Methods for details). The speleothem covers the time span from 9.6 to 6.1 kyr before present (BP). It can be divided into four sections exhibiting different growth rates ranging from 0.03 to 0.57 mm yr^{-1} (Fig. 1). Samples (826) for stable isotope measurements were drilled from the core by hand with an average sampling interval of 0.4 mm, yielding an average time resolution for the core of 4.1 years. For the fastest growth interval (high-resolution interval), however, between 7.9 and 8.3 mm yr^{-1}, the resolution increases to 1.4 years.

The $\delta^{18}O$ values vary between −4‰ and −6‰ VPDB, reflecting the characteristically low $\delta^{18}O$ of monsoonal rainfall[17] (Fig. 2a). The values of the upper 4 mm, which are not displayed in Fig. 2a, increase to −1.5‰, marking the end of the Holocene pluvial period. Modern stalagmites in this cave also have comparatively positive $\delta^{18}O$ ranging from 0‰ to −2‰, corresponding to the present arid climate[3]. Measurements of $\delta^{18}O$ of modern cave waters and actively

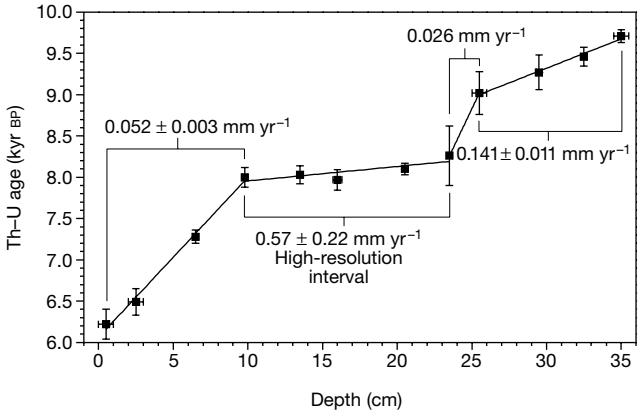

Figure 1 Plot of age versus depth for stalagmite H5. Twelve Th–U ages identify four sections with different growth rates varying between 0.03 and 0.57 mm yr^{-1}. All errors are 2σ (see Supplementary Information).

‡ Present address: Department of Geosciences, University of Massachusetts, Amherst, Massachusetts 01003, USA.